Use of Artificial Intelligence and Sizing and Simulation Software in Photovoltaic Plants

Carlos Eduardo Malaquias Fernandes[1*], Fernando Luiz Pellegrini Pessoa[1], Edson Ricardo Calado Sabino, Oberdan Rocha Pinheiro[1], Alex Álisson Bandeira Santos[1]

[1]SENAI CIMATEC University Center; Salvador, Bahia, Brazil

This academic study investigates the application of sizing and simulation software, such as PV*SOL and PVSYST, to analyze actual data collected from solar plants in Petrolina (PE), Messias (AL), and Piranhas (AL), comparing it with meteorological data from nearby stations. The study's objective is to assess the accuracy and effectiveness of these tools in implementing, testing, and monitoring solar plants. Essential factors in photovoltaic project design include meteorological data, site shading, module orientation, geographic location, temperature-induced losses, electrical components, equipment, and climate change considerations. The analysis covers January to December 2023, using hourly data from reliable meteorological inputs. These software tools aid in system sizing by incorporating multiple factors and estimating energy output, which is crucial to closely matching predicted energy production with actual performance. The quality of meteorological databases and mathematical models impacts software performance, necessitating efforts to filter, qualify, and catalog data sources. Production results indicated an annual output of 3,796 MWh for the Petrolina plant and 1,027 MWh for the Messias II plant, with measured data showing a 5% to 12% variation from estimated figures. Furthermore, the study incorporates Neural Designer, a machine learning-based neural network software, to conduct additional comparative analyses. The findings provide insights into site selection, equipment, plant characteristics, operational practices, and alignment of energy production with software predictions, offering recommendations for improvements and identifying potential locations for future solar farms.

Keywords: AI. Photovoltaic Plants. Brazil.

Photovoltaic generation (PVG) is marked by the inherent intermittency of solar resources, requiring careful management to ensure a stable electricity supply to the grid. Accurate PVG predictions can reduce the net cost of generation and contribute to grid security [1]. Solar forecasting minimizes the need for backup resources in energy imbalance markets, helping balance energy supply and demand [2].

Solar forecasting methods analyze the behavior of solar resources or PVG time series, using historical data from the series or other influencing factors to make predictions [3]. Solar forecasting techniques are classified into statistical, machine learning, physical, and hybrid approaches [4]. Machine learning models have gained prominence for hourly solar forecasting in recent years, and numerous studies have validated their effectiveness [5].

Received on 25 June 2024; revised 22 August 2024.

Address for correspondence: Oberdan Rocha Pinheiro. Avenida Orlando Gomes, 1845, Piatã. Salvador, Bahia, Brazil. Zipcode: 41650-010. E-mail: oberdan.pinherio@fieb.org.br.

J Bioeng. Tech. Health 2024;7(3):259-275

Photovoltaic plants experience predictable operational losses that impact performance, including ohmic losses in cabling [6], dust accumulation, light-induced degradation (LID) [7], and degradation over the module's lifespan, typically less than 1% per year [8]. Additional energy losses occur during the conversion from direct current (DC) to alternating current (AC) in the inverter [6].

Therefore, monitoring photovoltaic installations' energy output is essential to detect efficiency reductions caused by anticipated losses or environmental factors. For instance, a rainy year could reduce energy production due to diminished sunlight exposure rather than increased losses. Several parameters, including solar radiation on PV modules and ambient temperature, influence the energy output of a PV system [9]. Accurate, local data collection near the installation site is critical for making reliable predictions and ensuring an optimal return on investment [10].

Recognizing the need for metrics to improve efficiency and predictability in solar plants, this study utilizes artificial intelligence and statistical

and computational comparison methods to optimize renewable energy production and forecast performance. Integrating actual data with estimated results creates a database with diverse scenarios and plant types. This custom-architected software analyzes data through neural networks, aiding in predictive modeling. Over one year, the study provides insights that can help identify which locations will yield higher productivity, which months will generate the most energy, and much more, ultimately guiding investors and consumers on the optimal timing and location for installing solar power systems.

The photovoltaic cell operates based on the photovoltaic effect, utilizing semiconductor material, which has properties between a conductor and an insulator. Silicon, which visually resembles sand, is the primary semiconductor in the solar panels studied here. Pure silicon crystals lack free electrons, making them poor conductors. However, adding small amounts of other elements, a process known as doping enhances conductivity. When silicon is doped with phosphorus, the resulting material gains negatively charged free electrons, creating N-type silicon. Alternatively, doping with boron produces P-type silicon with positive charges. When N-type and P-type silicon are layered together (Figure 1), they form an electric field upon exposure to light, creating the environment necessary for the photovoltaic effect to occur. This effect enables the conversion of solar energy into electrical energy.

Types of Photovoltaic Panels

Monocrystalline Silicon (mono-Si) Cells: These cells use older technology but are highly efficient. They convert 14%–21% of sunlight into electricity. Their high efficiency allows for more energy generation per unit area, requiring less space than polycrystalline or thin-film cells.

Polycrystalline Silicon (poly-Si) Cells: Made from the same raw material as monocrystalline cells, poly-Si cells differ in crystal formation. They are produced by casting silicon into a block, making multiple crystals visible in each slice. This structure gives polycrystalline cells an efficiency of 13%–17%, slightly lower than monocrystalline cells.

Thin-Film Cells: Thin-film technology involves applying a layer of material, such as cadmium telluride (CdTe), copper indium gallium selenide (CIGS), or amorphous silicon (a-Si), to a flexible or irregular surface. Although their efficiency is lower (7–13%), they are more cost-effective and offer greater application flexibility.

Figure 1. Schematic of the photovoltaic effect on the silicon atom.

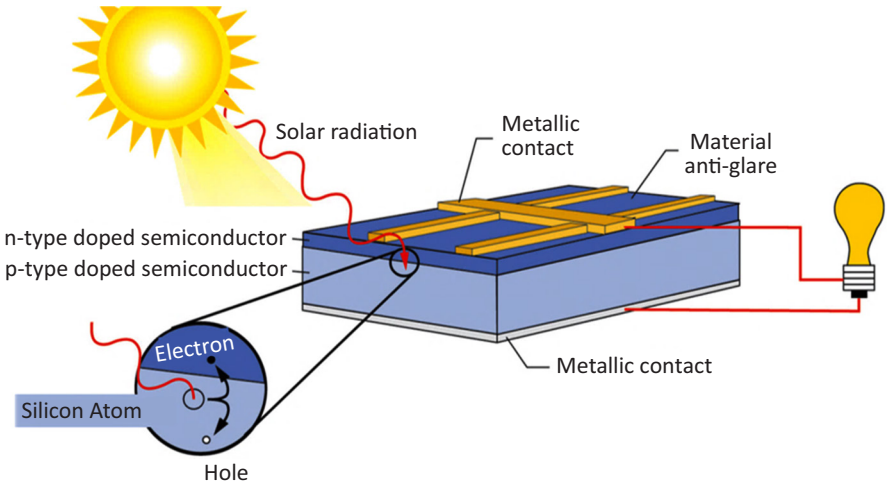

Components of a Solar Plant

Solar Panels: The core components that convert solar radiation into direct current (DC).

Charge Controllers: They regulate the charge in batteries, preventing overcharging or deep discharges and thus extending battery life.

Inverters: Often considered the "brain" of the system, inverters convert DC to alternating current (AC) and can raise voltage levels (e.g., from 12V to 127V). In some setups, inverters may connect to other generators or the grid.

Batteries: Acting as the system's "lungs," batteries store electricity for use when solar power is unavailable, such as during the night or on cloudy days.

Types of Photovoltaic Systems

Grid-Tied Systems: These systems connect to the electrical grid and can supply energy for general grid use. Unlike isolated systems, grid-tied systems do not require batteries or charge controllers, making them simpler and more efficient for a broad energy supply.

Off-Grid Systems: Isolated or autonomous, these systems are not connected to the grid. They directly power appliances and are generally designed for specific, local use.

Hybrid Systems: These systems combine photovoltaic energy with other power sources, such as wind turbines or diesel generators. Hybrid systems are versatile, as they can connect to the grid, operate in isolation, or be supported by the grid as needed.

Solar Potential in Brazil

Brazil's vast land area and extensive rooftop space in residential and commercial buildings, combined with high solar irradiance, present substantial potential for centralized and distributed solar generation. The Brazilian Solar Energy Atlas, published in 2017 by the National Institute for Space Research (INPE), indicates that the Northeast region has the highest average annual solar irradiation values (5.52 kWh/m² per day) and the lowest interannual variability [15]. This high irradiance, coupled with low precipitation and minimal cloud cover, especially in semi-arid areas, makes the Northeast a priority for solar energy investments, as evidenced by public and private projects.

Study Locations and Proposed Photovoltaic Plant

This study analyzes three locations: Petrolina (PE), Messias (AL), and Piranhas (AL), with Piranhas as a potential future site for photovoltaic projects. The planned plant will be located near Petrolina in an area designated as a Solar Energy Research Platform. Located along the São Francisco River, approximately 722 km from Recife in Pernambuco, Petrolina is a notable center for tourism and agricultural exports, especially fruits and wines. It has robust air and road infrastructure (including access via highways BR-232, BR-110, PE-360, BR-316, BR-428, and BR-122), as well as proximity to the Neoenergia (Companhia Energética de Pernambuco) 13.8kV distribution line, which is less than 100 meters from the project site at coordinates 9.39416° S, 40.5096° W.

The photovoltaic plant is situated in the São Francisco Pernambucano backlands, which features a tropical semi-arid climate (BSh). The terrain is flat with gently undulating features and typical caatinga vegetation adapted to the arid conditions. The soil is stony, with limestone and clay deposits. Historical meteorological data for the area indicate an annual average of 7.8 hours of sunshine per day, yielding approximately 5.38 kWh/m²/day (or 19.38 MJ/m²/day) in solar irradiation, an annual ambient temperature averaging 26.34°C, and an average annual rainfall of 538.7 mm.

Messias, located in Alagoas, spans 113.8 km² with a population of 17,856. The population density is about 156.9 inhabitants per km². Positioned 12 km Northeast of Rio Largo, Messias is bordered by Rio Largo, Murici, and Flexeiras. At an elevation of 104 meters above sea level, Messias experiences a tropical, hot, and humid climate with an average annual temperature of 24°C and rainfall of around 2,200 mm. The precipitation pattern is seasonal, with May, June, and July being the wettest months, while December through February are the driest.

Materials and Methods

Meteorological Data Collection Equipment (Table 1)

Critical for photovoltaic assessments, solar radiation data can be limited by location and measurement frequency. Solar radiation reaching the Earth's surface includes two primary components:

Direct Radiation: Sunlight that reaches the ground without deflection.

Diffuse Radiation: Sunlight scattered by atmospheric particles.

For precise solar resource assessment, both components are measured on inclined surfaces, such as photovoltaic (PV) modules. This data is gathered through specialized equipment, including pyranometers and pyrheliometers, which record solar radiation intensity. However, the cost of installing and maintaining these instruments at each distributed generation site is often prohibitively high (National Institute of Meteorology) [16]. These include:

Heliograph: Measures the duration of direct sunlight exposure (Figure 2A).

Actinograph: Continuously records solar energy reaching the area (Figure 2B).

Pyranometer: Accumulates the total solar energy incident throughout the day (Figure 3).

This advanced setup enables reliable data collection for energy modeling, ensuring that photovoltaic systems are accurately sized and capable of meeting their energy generation goals.

A pyrheliometer (Figure 3) measures direct solar irradiance. Sunlight enters the device through a window and is directed onto a thermopile, which converts the heat into an electrical signal. This signal's voltage is then processed using a specific formula to determine the irradiance in watts per square meter (W/m²) [11-14].

Table 1. Equipment present in the photovoltaic plant.

Instrument	Quantity	Variable
Anemometer	1	Wind direction and speed
Pyranometer First Class	2	Global solar radiation
Humidity sensor and temperature	1	Humidity and temperature

Figure 2A/B. Heliograph and Actinograph.

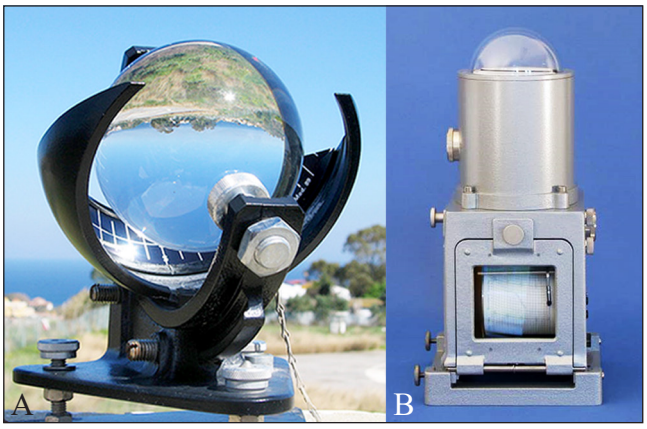

Figure 3. Pyranometer.

Climatological Stations at Solar Plants

Chef has established a climatological monitoring platform to improve data accuracy at the solar plants studied. This platform contains essential meteorological instruments for acquiring precise local data (Figure 4). The station complements government-run facilities by providing additional data and enabling a comprehensive regional analysis of solar resources. This setup assists in better understanding local climate patterns, ensuring a more accurate assessment of solar energy potential and operational efficiency at the plant locations.

The pyranometer (Figure 5) is a device used to measure solar radiation on a flat surface. It is designed to measure the density and solar radiation flux (W/m²) from the above hemisphere within a wavelength range of 0.3 μm to 3 μm.

Figure 4. Chesf climatological tower.

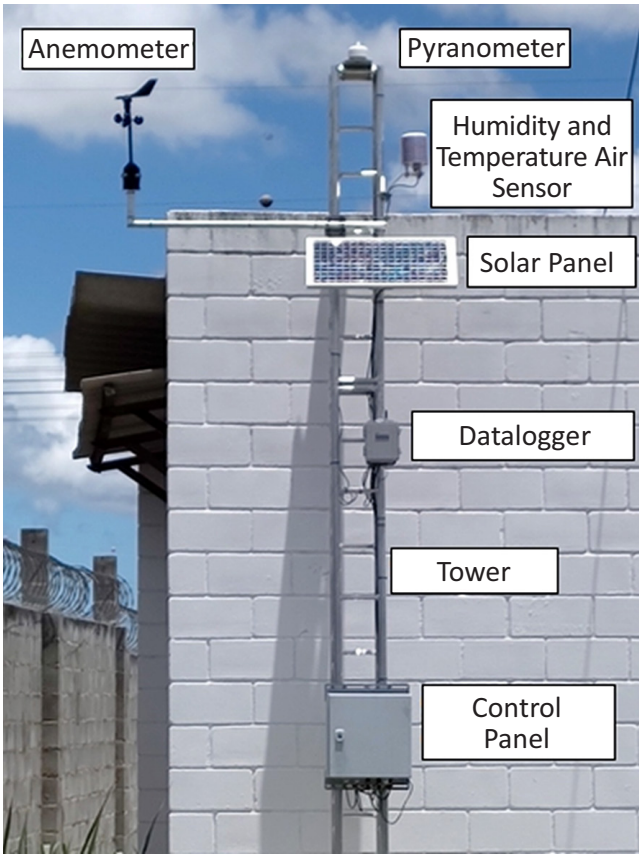

Figure 5. Pyranometer.

Other Data and Meteorological Sources

INMET (Instituto Nacional de Meteorologia) [15] and Partner Institutions: They provide access to meteorological products, allowing for the overlay of various data layers, such as satellite images, weather forecasting models, and severe weather alerts.

LABMET (Meteorology Laboratory): LABMET, the meteorology laboratory affiliated with the Federal University of Vale do São Francisco (UNIVASF), was established to support undergraduate and postgraduate courses. The laboratory also plays a crucial role in supporting agricultural activities in the region and providing the public with reliable information on weather and climate conditions. To achieve this, a state-of-the-art infrastructure was set up to monitor weather and climate variables and conduct agrometeorological research in the semi-arid region.

Global Solar Atlas (Solargis) [16]: The primary goal of the Global Solar Atlas is to offer quick and easy access to solar resource data and photovoltaic energy potential worldwide. It includes GIS layers and poster maps that showcase the resource potential on global, regional, and national scales.

Other Researched and Utilized Sources

- Meteonorm (used in Pvsol and Pvsyst for comparison);

- Copernicus Climate Atlas (for data comparison);
- Brazilian Solar Energy Atlas (for studies and analysis);
- Virtuxsolar (for observation of polarimetric data by latitude and longitude);
- CAMS Forecasts;
- CRESESB - Reference Center for Solar and Wind
- Energy Sérgio Brito;
- SUNDATA (CRESBES);
- UNESP - Agrometeorology and Solar Radiometry Laboratory (to observe solar ephemerides);
- Labren/Sonda/Redesolpe (for comparison studies).

Dimensioning and Simulation Software: To size a photovoltaic (PV) project, several factors must be considered, including ohmic losses, shading, module tilt angles, solar trajectory alignment, geographic location, and temperature-related power losses, as well as other electrical and climatic factors. Many of these are difficult to predict without the aid of a reliable meteorological database [17].

Given the numerous variables, photovoltaic simulation software can assist in the system sizing process by factoring in the considerations mentioned above. Such software should produce accurate results, as it is crucial to have a tool capable of predicting energy generation that closely matches the actual energy produced by an installed system.

The performance of this software also depends on the quality of the meteorological database and the mathematical models it employs [18].

Some commonly used software for PV system sizing include PVSYST [19] and PV*SOL [20]. It is important to note that these are paid tools, and Neural Designer will also be used for machine learning and neural network-based analysis. These software packages require annual fees or fixed costs for each version. Studies such as those by Machado and colleagues [21] and Silva and colleagues [22] have already compared the performance of the software mentioned (excluding SAM) with actual energy generation data from photovoltaic systems at various Chesf (Eletrobras) facilities in Petrolina - PE, Messias - AL, and Piranhas - AL.

The present study aims to compare PV*SOL and PVSYST by comparing simulation results with the actual energy outputs of the respective photovoltaic installations. This will allow for assessing the software's accuracy in forecasting energy production relative to actual system outputs in solar plants and determining whether the results are within the limits proposed in existing literature. PVSYST is widely recognized in academic and commercial sectors, making it an essential reference for this study.

For statistical analysis, the percentage difference between measured and estimated power will be calculated based on basic power calculations and the estimates produced by each software program included in the study.

Cell Output Power

Various factors, such as cell temperature, time of year, wind speed, ambient temperature, and geographical position, complicate accurately determining the energy production of a photovoltaic cell. Additionally, the efficiency of the cell (ηcell) decreases with increasing cell temperature, which directly impacts the output power (Pcell). Using the Total Power of Continuous Energy (PTEC) method, energy production can be estimated by integrating instantaneous generation over time for the module area, applying the formulas in Equations 1 and 2.

$$P_{cell,i} = A_{cell}\,\eta_{cell,i} G_i \qquad \text{Eq. 1}$$

$$Q_{pv,i} = A_{pv}\,G_i\,\eta_{eff,i}\,30 \qquad \text{Eq. 2}$$

Where:
- Apv or Acell = area of the PV plate (m²);
- ηcell, *i* = efficiency of the PV plate (%);
- *Gi* = solar radiation (W/m²);
- 30 = days of a month;
- i = number of months.

Period Analyzed, Qualification, and Data Filters

In this study, meteorological and radiation data were analyzed using data collected from both power generation and meteorological measurement equipment at Chesf (Eletrobras) solar plants involved in the research (Table 2).

The analyzed and proposed period is from 01/01/2023 to 12/31/2023, with hourly intervals of 01h (one hour), as made available by meteorological stations and downloaded from the INMET, LABMET system, and other meteorological data sources used in the study.

With a 13-hour analysis interval multiplied by 365 days for the year 2023, we will have 4745 data for each variant. Taking into account 7 to 8 variables studied, this totals a coverage of 33215 to 37960 items.

Another key aspect of the study was analyzing the locations of meteorological stations in relation to solar plants to enhance accuracy. Table 3 presents the respective distances.

Pre-treatment of Meteorological Data

It is recommended that the meteorological data selected undergo pre-treatment to ensure its quality and reliability. This process should include the following steps:

Time Filter: Select data from 05:00 to 18:00, corresponding to the solar cycle and the period of maximum usable radiation.

Data Cleaning: Filter out null, discrepant, and negative values within this time frame.

Missing Data Estimation: Apply the curve adjustment technique using averages for the specific period to estimate missing data.

File Preparation: Prepare CSV and TXT files for importing into the applications used in this study.

Software Data Analysis: Some tested software tools include interfaces that analyze the imported data.

Literature Review: Further investigation of related data and literature can help refine the analyzed

These tools generate logs and alert or error messages if null, discrepant, or erroneous data is detected. Sometimes, the software identifies the problematic

Table 2. Geoclimatic information on photovoltaic plants.

Location	Altitude (m)	Cloudiness Annual Average (tenths)	Rains (mm)	Climate
Petrolina	385	0.5	430	Semiarid
Messias	104	0.5	777	Tropical Rainy
Piranhas	88	0.5	492	Tropical

Table 3. Station identification and station distance photovoltaic plant.

Location	Station Chosen	Distance from the Station by the Plant (Km)
Petrolina	LABMET/CHESF	23
Messias	INMET/UFAL/CHESF	12
Piranhas	INMET/UFAL	4

data, prompting the user to review and correct it. meteorological data source.

Solar Plant Location Suggestion in Piranhas (AL)

For selecting the location of the solar plant within the Chesf (Eletrobras) facilities' territorial area, the following criteria were considered:

- **Proximity to Electrical Infrastructure**: The site should be close to existing electrical installations within the Chesf (Eletrobras) network.
- **Proximity to Meteorological Stations**: The location should be near a meteorological station or a research center focused on meteorology.
- **Radiation Levels and Feasibility**: The site should have favorable radiation rates to implement a photovoltaic system.
- **Accessibility**: The site should be easily accessible and ideally located near a medium-sized city, facilitating labor availability, construction, and commissioning.
- **Educational and Research Opportunities**: The presence of technical or higher education institutions nearby could provide qualified labor and allow the plant to serve as a reference for academic studies. Expanding knowledge areas and Chesf (Eletrobras) would benefit the educational institution by developing human capital and expertise.

Methodology for Location Selection

In addition to the factors outlined above, the Brazilian Solarimetric Atlas (Version 2000) – Cresesb was used, focusing on the areas of Piranhas (AL) and Canindé do São Francisco (SE), near the Chesf (Eletrobras) complex in Xingó.

Three potential points of interest were identified with the support of the Global Solar Atlas (Solargis) platform. These points were selected based on their distance to the local meteorological station and the Chesf facility (Substation SE Xingó 69 kV). They are referred to as Point 1, Point 2, and Point 3.

Another critical aspect of the research was investigating the nearby meteorological stations, assessing their data collection capabilities, and evaluating their operational status.

Results and Discussion

During this work, the broad possibilities of using sizing, simulation, and neural network software for use in photovoltaic plants were emphasized, especially Cresp solar plants – Solar Energy Reference Center of Petrolina (PE), Messias II (AL) and as a suggestion, a possible design and implementation of a solar plant in the city of Piranhas (AL), as this location has Chesf (Eletrobras) facilities.

This section addresses the methodological procedures for comparing and evaluating the use of global solar irradiation (GHI) databases obtained through INMET, Labmet, and other meteorological sources and validating their use in solar energy systems.

The methodology continues to obtain global solar irradiation data from the two databases for the chosen cities and compare them using graphs and statistical indicators. These cities were selected because they have local meteorological stations and solar plants from Chesf (Eletrobras).

As sensors are susceptible to errors, some radiation or meteorological information may not be in the bank. Therefore, a broader data search is carried out.

Measurement Data

Cresp Photovoltaic Plant – Petrolina (PE)

Data from the Cresp Petrolina solar plant were collected, and an online database was downloaded from the SCADA WEG software platform (Table 4).

Photovoltaic Plant – Messias (AL)

In the Messias II plant, data from the GOODWE platform shows that the total output comes from

seven inverters, each with a 25 kW capacity, though one inverter is currently offline, resulting in an active output of six inverters at 100 kW each. According to the project's descriptive memorandum and calculations (Resende [23]), technical specifications of the modules and inverters are outlined. Simulations run in PVSyst software (version 6.35) estimate an annual energy generation of 1.431 MWh for the designed system (Table 5).

Table 6 summarizes all the meteorological variables used in the study and in the three locations observed, considering their monthly average.

In Table 7, we can observe the GHI and LAT values for the studied locations. Below, we have the explanatory legend of these types of radiation. It is worth noting that in this present study, we focused on the two types of radiation due to their particularities and uses in the academic and project fields.

Table 4. Generated energy Petrolina (PE).

	2020	2021	2022	2023
Real Energy (MWh)	3428.77	3822.51	3467.34	3796.64

Table 5. Generated Energy Messias (AL).

	2020	2021	2022	2023
Real Energy (MWh)	122.67	72.51	107.08	118.19

Table 6. General table of meteorological data.

		Jan	Febr	Mar	Apr	May	Jun	Jul	Aug	Sep	Oct	Nov	Dec
Petrolina	**Temp. °C**	28	28	28	27	27	25	25	25	27	28	29	28
	Rain mm	62,8	80.2	101.7	49.5	8	4.6	3	1.8	3.3	11.1	45.8	63.8
	KT Index	42.4	48.9	46.8	40.6	38.6	38.2	41.3	31.3	24.6	25.4	47.4	42.9
	Humidity %	58	63	67	70	64	61	60	53	48	48	50	54
	Wind Km/h	23.4	21.4	20.5	20.6	22.4	23.6	25.4	26.4	25.4	24.2	22	21
Messias	**Temp. °C**	26	27	27	26	25	24	23	23	24	25	26	26
	Rain mm	18.1	23.2	44.5	131.3	199.8	199.6	199.2	52.7	22.7	28.2	11.4	13.3
	KT Index	37.6	33	37.3	37.2	48.8	49.3	49.3	52.6	47.2	41.4	39.8	40
	Humidity %	75.9	70.4	66.9	78.5	84.9	75.4	65.1	75.8	83.6	82.1	79	78.7
	Wind Km/h	24.8	23.6	20.9	19.8	18.8	21	21.5	23.1	22.2	24.1	26.8	25.4
Piranhas	**Temp. °C**	29	29	29	28	26	25	24	24	26	28	29	29
	Rain mm	34.3	40.4	53.3	61.8	71.3	60.3	58	27.8	14.7	12.8	22.3	38.8
	KT Index	40.3	37.8	32.9	45.2	37.4	33.9	35.3	38.8	37.2	47.5	60.2	54.3
	Humidity %	53.1	52.1	57.8	66.9	76.2	78.6	78.5	72.5	67.8	61.7	64.5	62.6
	Wind Km/h	24.1	23.8	22.6	18.9	17.5	18.4	19.8	22.2	24.7	28.9	27.2	27.7

GHI: Global Horizontal Irradiation; LAT: Global irradiation at the tilt of the local latitude.

Table 7. GHI and LAT comparison in the 3 locations (kWh).

	Petrolina		Messias		Piranhas	
Irrad.	**GHI**	**LAT**	**GHI**	**LAT**	**GHI**	**LAT**
Anual	5.76	5.78	5.22	5.22	5.47	5.47
Jan	6.38	6.00	5.87	5.53	6.31	5.94
Feb	6.16	5.96	5.83	5.64	6.06	5.86
Mar	6.02	6.03	5.84	5.85	5.97	5.98
Apr	5.24	5.44	5.06	5.25	5.32	5.53
May	4.82	5.16	4.23	4.52	4.47	4.78
Jun	4.57	4.97	3.90	4.21	4.07	4.41
Jul	4.82	5.19	4.00	4.30	4.20	4.51
Aug	5.55	5.84	4.57	4.79	4.83	5.08
Sep	6.32	6.4	5.39	5.45	5.66	5.73
Oct	6.40	6.24	5.67	5.53	5.96	5.81
Nov	6.50	6.16	6.16	5.84	6.43	6.09
Dec	6.38	5.95	6.11	5.70	6.36	5.93

We cannot forget the chosen arrangement and the results obtained by the Neural Network using the Neural Designer software (Table 8).

Figure 6 shows a graphical representation of the network architecture.

Although this paper focuses on comparisons between measured and estimated energy production, we have added a goodness-of-fit plot between the

Table 8. Perceptron framework.

Perceptron Layer	Number of Entries	Number of Neurons	Activation Function
1	6	3	Hyperbolic Tangent
2	3	1	Linear

Figure 6. Neural network model.

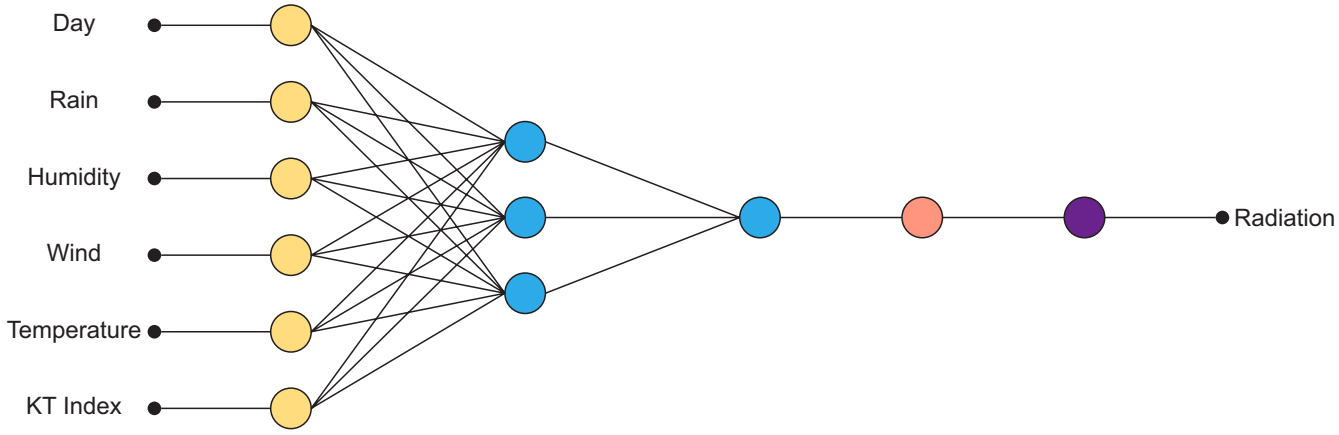

Scaling layer with 6 neurons (yellow; perceptron layer with 3 neurons (blue); perceptron layer with 1 neuron (blue; de-scaling layer with 1 neuron (red); bounding layer with 1 neuron (purple).

same variables to demonstrate how well a statistical model fits a set of observations. Goodness-of-fit measures are used to measure the discrepancy between observed values and expected values under a probability model (Figures 7 and 8).

Table 9 below shows the data arrangement, number of samples, and percentages of samples chosen for each stage of the neural network calculations.

Concerning the proposed location of a plant in the Piranhas region (Alagoas), results from the three observed points are presented as follows. Another key aspect of the research involved identifying nearby meteorological stations, assessing data availability at these sites, and evaluating their operational status. To support this, the Atlas Solar Global platform (Solargis) was utilized, enabling measurement and sizing on an embedded map. Using this platform, three specific points of interest were selected (Figures 9-11).

The website (Forensically Beta, 2024) facilitates uploading saved images for analysis. Once the image is uploaded, it appears on the main screen. By selecting the "Level Sweep" tab and applying the adjustments shown in the image below, the darkest points on the polarimetric map section are highlighted. This step helps identify areas with the highest irradiation levels (Figure 12).

Table 10 presents the results for the three points, with a particular emphasis on point 3, where the sample shows the best results aided by the Global Solar Atlas.

Tests were conducted using PVSYST, PVSOL, and Neural Designer software, with estimated radiation values calculated from both measured and projected data. Following this, the comparison

Figure 7. Estimated and measured radiation - Goodness of Fit Cresp Petrolina in kWh.

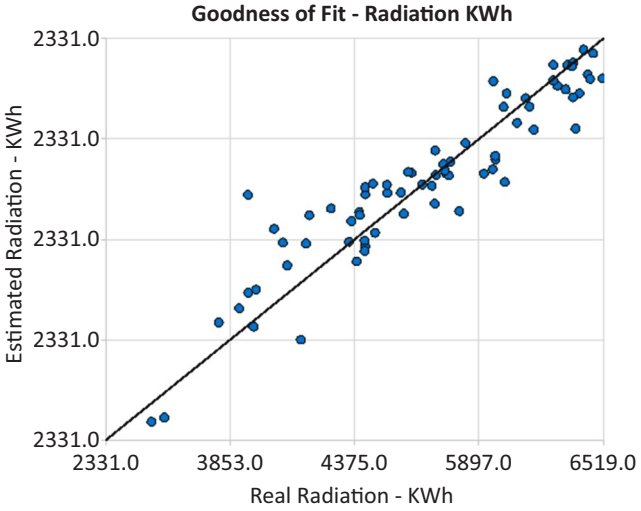

Figure 8. Estimated and measured radiation - Goodness of Fit Messias in kWh.

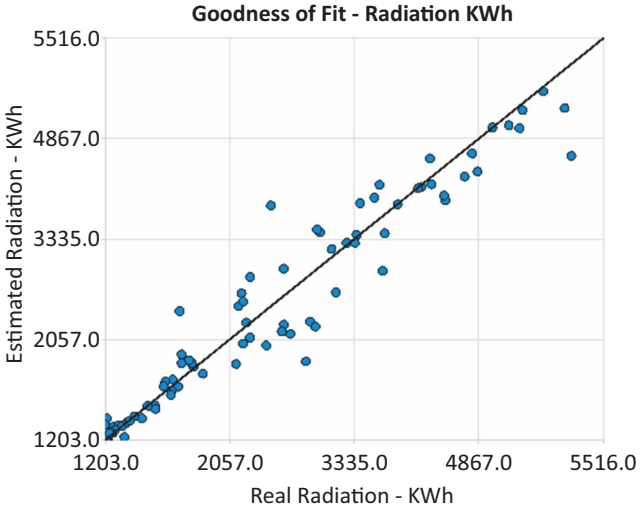

Table 9. Sample chart.

	Petrolina	Messias	Piranhas	% Samples
Training Samples	2697	2441	2248	60%
Selection Samples	899	813	749	20%
Test Samples	899	813	749	20%
Unused samples	0	0	0	0%

Figure 9. Point 1: Close to Canindé do São Francisco, next to the substation (SE Xingó 69 kV) - location: 9°37'37.1 "S 37°48'41.0".

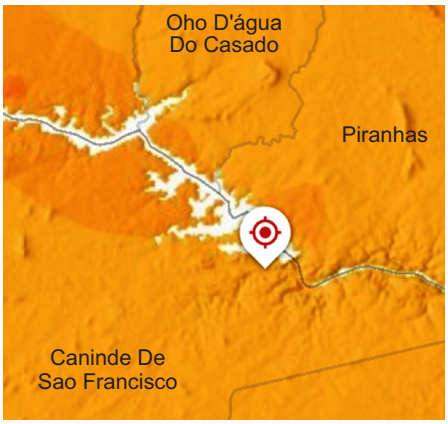

Distance from the fictitious photovoltaic plant Point 1, to the Inmet Piranhas A371 station, located next to UFAL Instituto Federal de Alagoas, Piranhas Campus: 4.90 Km.

Figure 10. Point 2: Nearby Piranhas AL aerodrome - location: 09°34'48" s, 37°47'02 "w.

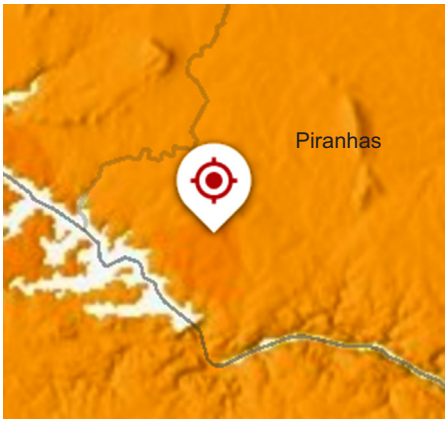

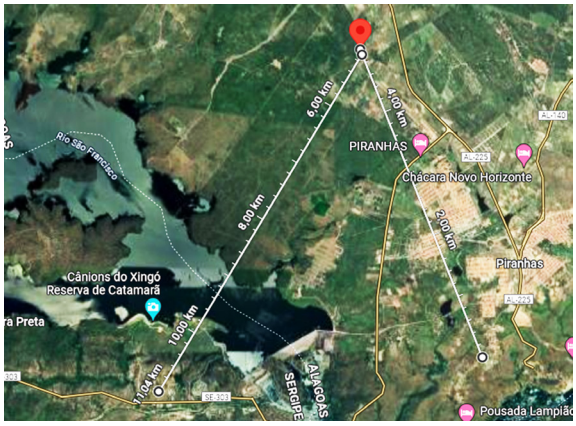

The distance to INMET PIRANHAS A371 station, located next to UFAL Instituto Federal de Alagoas, Piranhas Campus, is 5.00 km.Distance from the Ponto 2 photovoltaic plant to the SE Xingó 69kV Chesf substation (Eletrobras): 6.00 Km.

Figures 11. Point 3: Close to the Lameirão settlement in the municipality of Delmiro Golveia in Alagoas - location: 9°30'53.0 "S 37°58'50.0 "W.

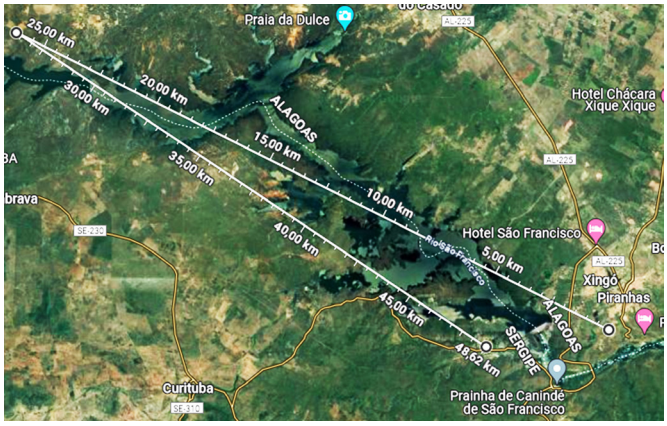

The distance to INMET PIRANHAS A371 station, located next to UFAL Instituto Federal de Alagoas, Piranhas Campus, is 26.22 km. Distance from the Ponto 3 photovoltaic plant to the SE Xingó 69kV Chesf substation (Eletrobras): 22.4 Km.

Figure 12. Forensically beta site to search for points with the highest radiation.

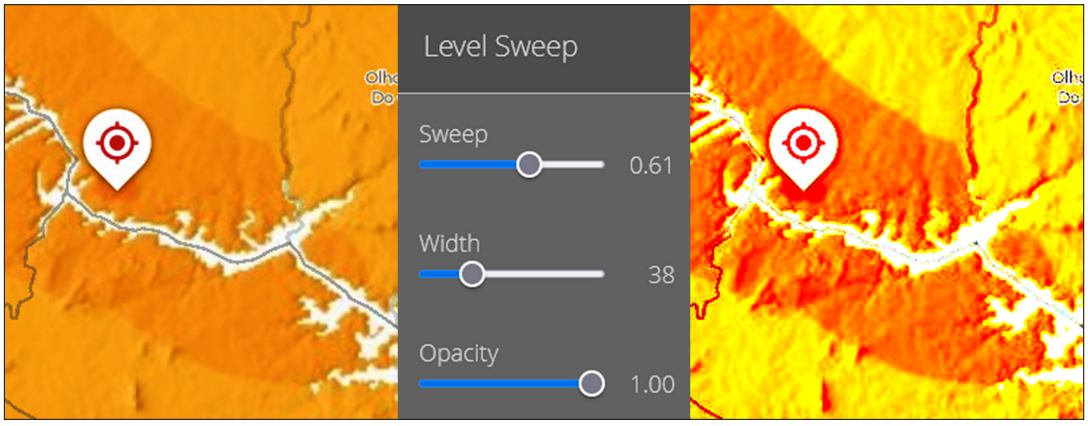

Table 10. Comparative data simulated by Atlas Solar Global in the 3 points.

Index	Acronym	Point 1	Point 2	Point 3	Unit.
Specific Photovoltaic Power	PVOUT	4.352	4.397	4.535	kWh/kWp day
Normal Direct Irradiation	DNI	4.451	4.476	4.870	kWh/m² day
Global Horizontal Irradiation	GHI	5.543	5.559	5.749	kWh/m² day
Diffuse Horizontal Irradiation	DIF	2.356	2.364	2.247	kWh/m² day
Global Irradiation Tilted at Optimal Angle	GTI_opta	5.589	5.611	5.803	kWh/m²
Air temperature	TEMP	26,9	25.8	25.9	°C
Optimal Tilt of Photovoltaic Modules	OPTA	8	9	9	° degrees
Terrain Elevation	ELE	69	249	221	m

percentages for the total radiation measured at the modules' inverter were determined. Tables 11, 12, and 13 display these comparisons for the locations of Petrolina (PE), Messias (AL), and the proposed plant site in Piranhas (AL). Note that Piranhas (AL) participates only in calculations using Neural Designer, as it is a suggested location without direct measurement data.

Conclusion

The most significant challenge during this research was acquiring complete, cohesive, and high-quality data. However, success was achieved after an extensive review of multiple data sources, enabling the selection of the most reliable and comprehensive datasets. The data qualification and filtering stage followed, ensuring accuracy. Despite this, a lack of standardization, insufficient data, and inadequate meteorological stations remain significant issues. Many operational stations either do not provide all the necessary data or experience periods of inactivity. While Brazil boasts a network of meteorological stations, many regions still face gaps in monitoring coverage.

Three locations in the Northeast were analyzed, each exhibiting distinct climatic characteristics. For example, Messias (AL) experiences higher precipitation rates of 944 mm, almost double the averages of the other two locations: Petrolina (PE)

Table 11. Radiation results in software and their percentages for Petrolina in kWh.

PETROLINA in kWh								
	Estimated	**Real**	**PVSYST**	**PVSOL**	**NEURAL**	**% PVSYST**	**% PVSOL**	**% Neural Network**
Jan	127.15	127.02	181.58	160.71	165.22	42.95	26.52	30.07
Feb	126.68	117.11	138.64	138.80	131.29	18.38	18.52	12.11
Mar	116.05	119.26	162.80	135.44	134.91	36.51	13.57	13.12
Apr	109.13	125.40	137.16	114.43	108.87	9.38	-8.75	-13.19
May	92.01	106.24	104.67	100.90	111.31	-1.48	-5.02	4.77
Jun	94.13	102.87	94.18	92.73	108.12	-8.44	-9.85	5.11
Jul	120.95	138.51	103.15	99.27	121.93	-25.53	-28.33	-11.97
Aug	131.04	138.42	123.48	124.74	144.45	-10.79	-9.88	4.36
Sep	145.51	141.72	145.49	144.91	149.25	2.66	2.25	5.31
Oct	153.65	152.26	157.89	164.36	153.34	3.70	7.95	0.71
Nov	143.21	122.05	167.90	159.40	161.71	37.57	30.60	32.50
Dec	142.47	122.97	156.94	160.81	157.18	27.62	30.77	27.82
Annual	1501.98	1513.82	1673.88	1596.51	1647.59	10.57	5.46	8.84

Table 12. Radiation results in software and their percentages for Messias (AL) in kWh.

MESSIAS II in kWh								
	Estimated	**Real**	**PVSYST**	**PVSOL**	**Neural**	**% PVSYST**	**% PVSOL**	**% Neural Network**
Jan	132.84	111.65	130.40	136.47	151.38	16.79	22.23	35.59
Feb	114.73	95.96	113.10	125.10	130.31	17.86	30.36	35.80
Mar	121.97	109.10	111.10	121.59	139.15	1.83	11.45	27.55
Apr	102.57	95.93	101.90	102.14	117.04	6.22	6.47	22.01
May	92.13	89.71	88.10	90.08	105.13	-1.79	0.41	17.19
Jun	76.22	68.70	69.90	81.70	86.97	1.75	18.93	26.60
Jul	85.18	88.51	81.10	85.32	97.18	-8.37	-3.60	9.80
Aug	98.30	86.91	97.80	103.43	112.16	12.53	19.01	29.06
Sep	101.81	89.34	107.70	116.17	115.99	20.55	30.03	29.83
Oct	119.85	102.11	123.00	133.82	135.53	20.46	31.06	32.73
Nov	104.48	62.70	130.10	141.03	119.45	107.50	124.93	90.50
Dec	125.86	27.20	136.80	141.21	143.38	402.94	419.15	427.13
Annual	1275.94	1027.82	1291.00	1378.07	1453.69	25.61	34.08	41.43

Table 13. Estimated radiation percentage x neural designer radiation in Piranhas plant.

	Jan	Feb	Mar	Apr	May	Jun	Jul	Aug	Sep	Oct	Nov	Dec	Annual
Estimated	168	150,7	153,5	142,3	115,1	105,6	150,2	152,2	174,2	162,9	168,06	154,2	1797
Neural	151,4	132,9	134,1	124,3	100,6	94,98	131,2	132,9	153,4	149,3	154,91	138,1	1598
% Neural Network	-9,86	-11,8	-12,6	-12,6	-12,6	-10,1	-12,6	-12,6	-12	-8,4	-7,82	-10,41	-11,1

with 435 mm and Piranhas (AL) with 495 mm. The proximity of the São Francisco River in Piranhas may cause a microclimate, which could positively or negatively affect the data obtained.

As for temperature, the annual average remained consistent across all three cities, with Messias (AL) recording 25.16°C and Petrolina (PE) and Piranhas (AL) averaging around 27°C. The cloudiness index in Messias (AL) and Piranhas (AL) was similar at around 42%, whereas Petrolina had a slightly lower index of 39%. Regarding humidity, Messias (AL) had 76%, Petrolina (PE) 58%, and Piranhas (AL) 66%. The average wind speed across all locations was approximately 23 m/s. These data are crucial for a broader understanding of the plant's potential. Minor shading in the study areas was noted but did not affect the overall results.

As observed by Iea-Pvps [24], dirt and other loss factors were also considered in the calculations, leading to an annual loss of 3% to 4%, reaching up to 7% in some cases, by standards set by IEA-PVPS (International Energy Agency Photovoltaic Systems Programme). Regarding irradiation, higher values were observed at the Petrolina (PE) plant, with an annual average of 5.76 kWh, while Piranhas recorded 5.47 kWh and Messias 5.22 kWh. This variation in irradiation was reflected in energy production: Petrolina (PE) produced between 1501 and 1673 kWh/year per m², Piranhas (AL) between 1597 and 1796 kWh/year per m², and Messias (AL) between 1027 and 1453 kWh/year per m². When comparing measured energy production to estimated values, the results were positive and within acceptable tolerances. In Petrolina (PE), energy production was 5.46% higher than measured values in PVSOL, 8.84% higher in Neural Designer, and 10.57% higher in PVSYST.

The differences in Messias (AL) were more significant, with energy production in PVSYST being 25.61% higher, PVSOL 34% higher, and Neural Designer 41.43% higher. When accounting for the decrease in production during October, November, and December, replacing the lower values with historical averages, the percentage differences were reduced to 12.4% in PVSYST, 20.4% in PVSOL, and 26.7% in Neural Designer.

The proposed solar plant in Piranhas (AL) showed promising results, with three potential installation sites identified: Piranhas (AL), Delmiro Gouveia (AL), and Canindé do São Francisco (SE). These sites were selected for their proximity to a meteorological station, the Federal University of Alagoas (UFAL) advanced campus, and several Chesf (Eletrobras) facilities.

The difference between estimated and calculated energy production from the software was approximately 11%, with the potential for further reduction depending on the selected installation point. In evaluating the software, it became evident that each tool has strengths and unique features.

The results were generally consistent, with some software offering additional functions and a broader database, while others required a better understanding of data entry and technical aspects. PVSOL stands out for its 3D project visualization capabilities, whereas PVSYST focuses more on technical aspects and reporting. Both software options offer significant flexibility in input parameters, including a wide range of equipment manufacturers in the solar energy sector, which aids in obtaining accurate results. PVSYST and PVSOL allowed testing of different module tilt angles, concluding that the chosen angle for the project is the most efficient and cost-effective.

Neural Designer's application in the electrical sector shows promise, though it is more widely used in various commercial and industrial fields.

The Neural Designer yielded positive results in the tests conducted, though it required clean data with minimal discrepancies. Despite this initial challenge, the software demonstrated good performance, offering high customizability and the ability to predict various outputs and prognoses. This study provided valuable insights into the potential for photovoltaic energy production in the Northeast region of Brazil, and the findings have implications for future solar plant installations in the area.

Acknowledgment

The authors would like to express their sincere gratitude to SENAI CIMATEC for its support and provision of researcher resources that significantly contributed to the success of this project.

Furthermore, the authors also thank the Research and Development Program of the Brazilian electricity sector regulated by ANEEL and Eletrobras CHESF for the financial support and all the employees and collaborators at Chesf (Eletrobras) who helped me in some way with this project.

References

1. Lima MAFB, Carvalho PCM, Fernández-Ramírez LM, Braga APS. Improving solar forecasting using deep learning and portfolio theory tntegration. Energy 2020;195:117016.
2. Wang GC, Ratnam E, Haghi HV, Kleissl J. Corrective receding horizon EV charge scheduling using short-term solar forecasting. Renewable Energy 2019;130:1146–1158.
3. Carneiro TC, Santos HAD, Braga APDS, Carvalho PCMD. Redes neurais artificiais para previsão de velocidade do vento: estudo de caso para Maracanaú–CE. Congresso Brasileiro de Automática 2014.
4. Antonanzas J, Osorio N, Escobar R, Urraca R, Martinez-De-Pison FJ, Antonanzas-Torres F. Review of photovoltaic power forecasting. Solar Energy 2016;136:78–111.
5. Mertyagli G, Yang D, Srinivasan D. Automatic hourly solar forecasting using machine learning models. Renewable Sustainable Energy Rev 2019;105:487–498.
6. Nascimento LMA, Ferreira RAF. Otimização de um sistema fotovoltaico conectado à rede elétrica: considerações sobre a eficiência do sistema e análise de posicionamento. Revista de Engenharia e Tecnologia.v.10, N° 3. Dez/2018.
7. Silva IND, Spatti DH, Flauzino RA. Redes neurais artificiais para engenharia e ciências aplicadas. 1. ed. São Paulo: Artliber, 2010.
8. Cassini DA, Oliveira MCC, Soares LG, Viana MM, Lins VFC, Diniz ASAC, Zilles R, Karmerski LL. Avaliação do desempenho da degradação de módulos fotovoltaicos de Si cristalino após 15 anos de exposição em campo. In: VIII Congresso Brasileiro de Energia Solar - CBENS, RS 2018.
9. Carneiro TC, Santos HAD, Braga APDS, Carvalho PCMD. Redes neurais artificiais para previsão de velocidade do vento: estudo de caso para Maracanaú–CE. Congresso Brasileiro de Automática 2014.
10. Murat Ates A, Singh H. Rooftop solar photovoltaic (PV) plant – One year measured performance and simulations. Journal of King Saud University - Science 2021;33(3):101361.
11. Marques ICA, Delvizio ES. Estudo de viabilidade técnica de microgeração residencial fotovoltaica. Revista Científica Multidisciplinar Núcleo do Conhecimento 2020;5(3):166-203
12. Wang H, An C, Duana M, Su J. Transient thermal analysis of multilayer pipeline with phase change material. Appl Ther Eng 2020;165:114512.
13. Montgomery DC, Jennings CL, Kulahci M. Introduction to time series analysis and forecasting. ed.: John Wiley & Sons 2015.
14. Quadros FSD. Sistema de Divulgação de Dados Meteorológicos. 2005. 105 p. (Doutorado). Centro de Ciências Tecnológicas da Terra e do Mar, Universidade do Vale do Itajaí 2005.
15. Pereira EB, Martins FR, Gonçalves AR, Costa RS, Lima FJL et al. Atlas brasileiro de energia solar. 2a. ed. São José dos Campos: INPE, 2017. Available at: http://labren.ccst.inpe.br/atlas_2017.html .
16. Scolar J, Martins D, Escobedo JF. Estimativa da irradiação total sobre uma superfície inclinada a partir da irradiação global na horizontal. Revista Brasileira de Geofísica, v.21, n.3, p.249-258, 2003. http://www.scielo.br/pdf/rbg/v21n3/a04v21n3.pdf.
17. Oliveira LGM. Avaliação de fatores que influenciam na estimativa da geração e operação de sistemas fotovoltaicos conectados à rede elétrica, Tese de Doutorado, Universidade Federal de Minas Gerais, Belo Horizonte 2017.
18. Rosa VB. Aplicação Computacional para o Dimensionamento de Sistemas Fotovoltaicos Isolados, Trabalho de Conclusão do Curso, Escola Politécnica da Universidade Federal do Rio de Janeiro, Rio de Janeiro 2014.

19. Pvsyst, Photovoltaic Software features, 2023. Available at: https://ww.pvsyst.com/features/.
20. Pvsol, Pv*Sol Valentim Software, 2023. Available at: https://valentin-software.com/en/products/pvsol-premium/.
21. Machado CT, Miranda FS. Energia Solar Fotovoltaica: uma breve revisão. Rev Virtual Quim 2015;7(1):126-143.
22. Silva JL et al. A Comparative performance of PV power simulation software with an installed PV plant. IEEE International Conference on Industrial Technology (ICIT), São Paulo, Brasil 2020:531-535. doi: 10.1109/ICIT45562.2020.9067138.
23. Resende Degs M. Implantação de sistema de geração fotovoltaica 700kw subestação de Messias II. Recife: Chesf, 2021:45.
24. Iea-Pvps, Soiling Losses – Impact on the Performance of Photovoltaic Power Plants 2022. Available at : https://iea- pvps.org/ wp-content/uploads/2023/01/IEA-PVPS-T13-21-2022-REPORT-Soiling-Losses-PV-Plants.pdf.